Electronic Supplementary Material (ESI) for Journal of Materials Chemistry C.

Supporting Information

Classification of MAOX Phases and Semiconductor Screening for Next-Generation Energy Conversion Ceramic Materials

Zhenyu Wang,[a,†] Xin Chen, [a,†,] and Chunming Niu [a,*]*

*Center of Nanomaterials for Renewable Energy (CNRE), State Key Lab of Electrical Insulation and Power Equipment, School of Electrical Engineering, Xi'an Jiaotong University, 99 Yanxiang Road, Xi'an 710054, China.*E-mail: xin.chen.nj@xjtu.edu.cn; cniu@xjtu.edu.cn;*
†Author Contributions Zhenyu Wang, Xin Chen: Equal author contributions.

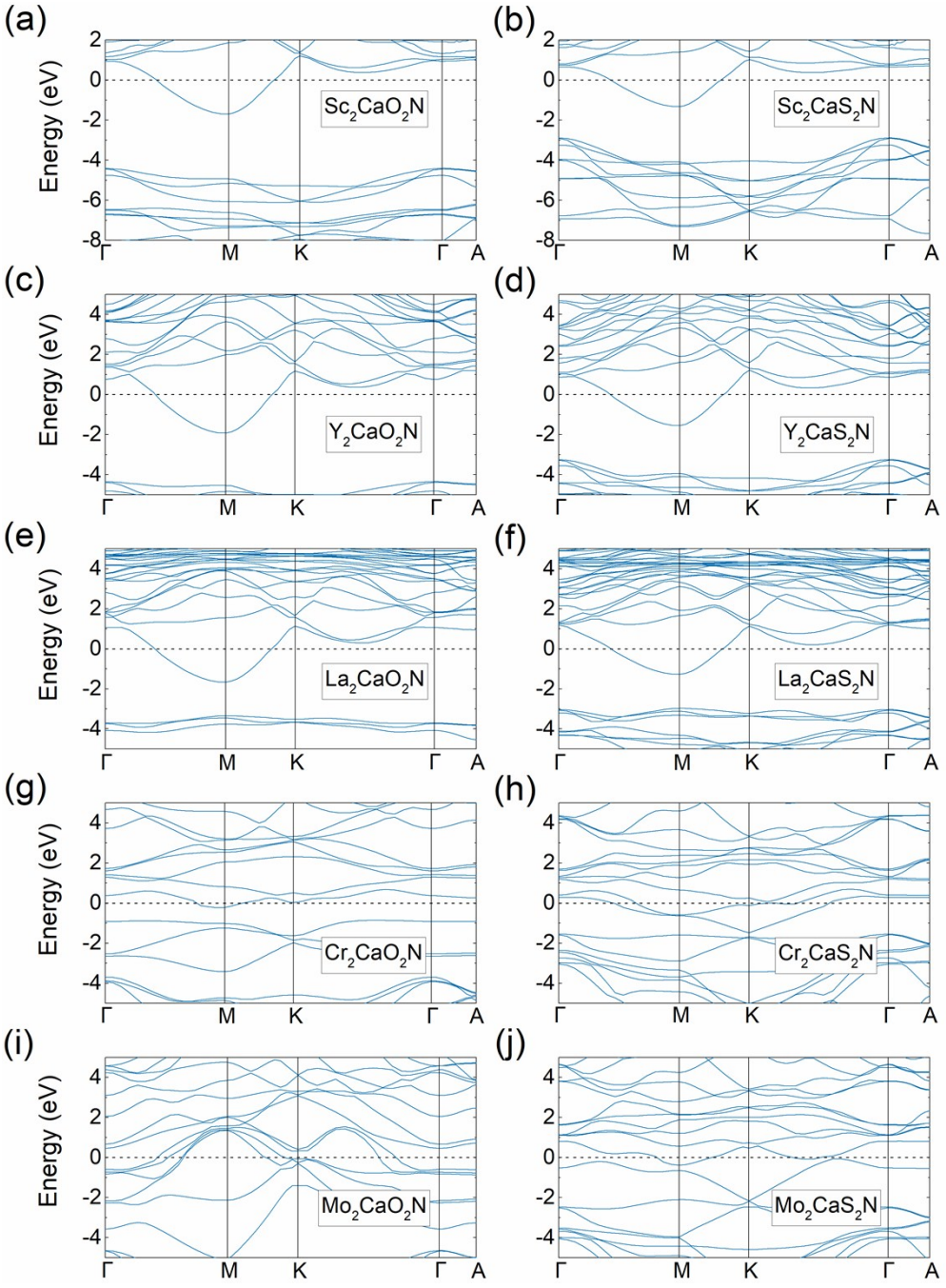

Figure S1. Band structures of the oxynitride and sulnitride MAOX: (a) Sc_2CaO_2N, (b) Sc_2CaS_2N, (c) Y_2CaO_2N, (d) Y_2CaS_2N, (e) La_2CaO_2N, (f) La_2CaS_2N, (g) Cr_2CaO_2N, (h) Cr_2CaS_2N, (i) Mo_2CaO_2N and (j) Mo_2CaS_2N. The black dash line indicates the Fermi level.

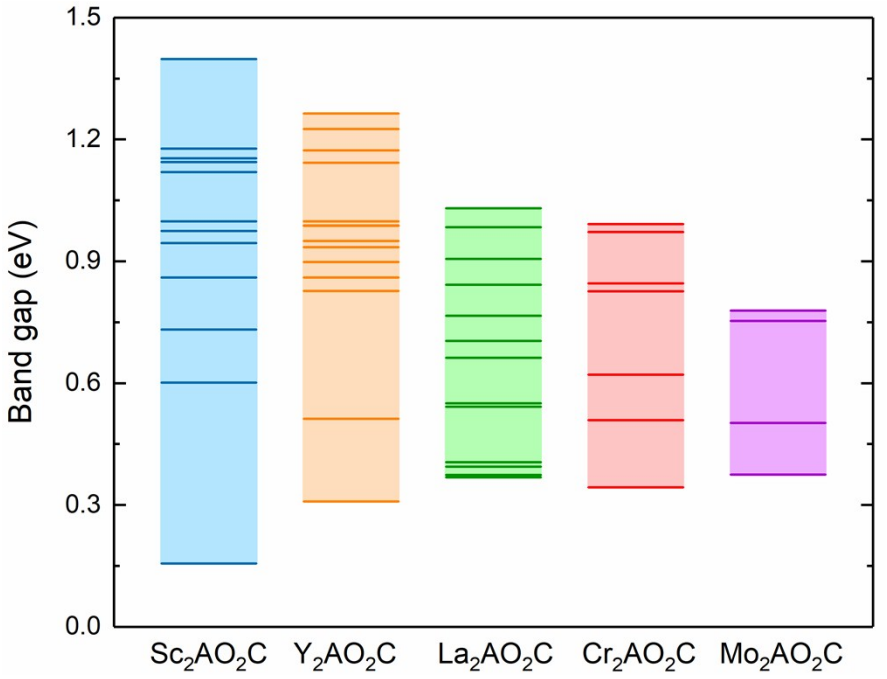

Figure S2. Bandgap distribution of MAOX semiconductor sorted by M, where the shadow indicates the distribution range, where A=Be, Mg, Ca, Sr, Ba, Cu, Zn, Cd or Hg, and O=S or O.

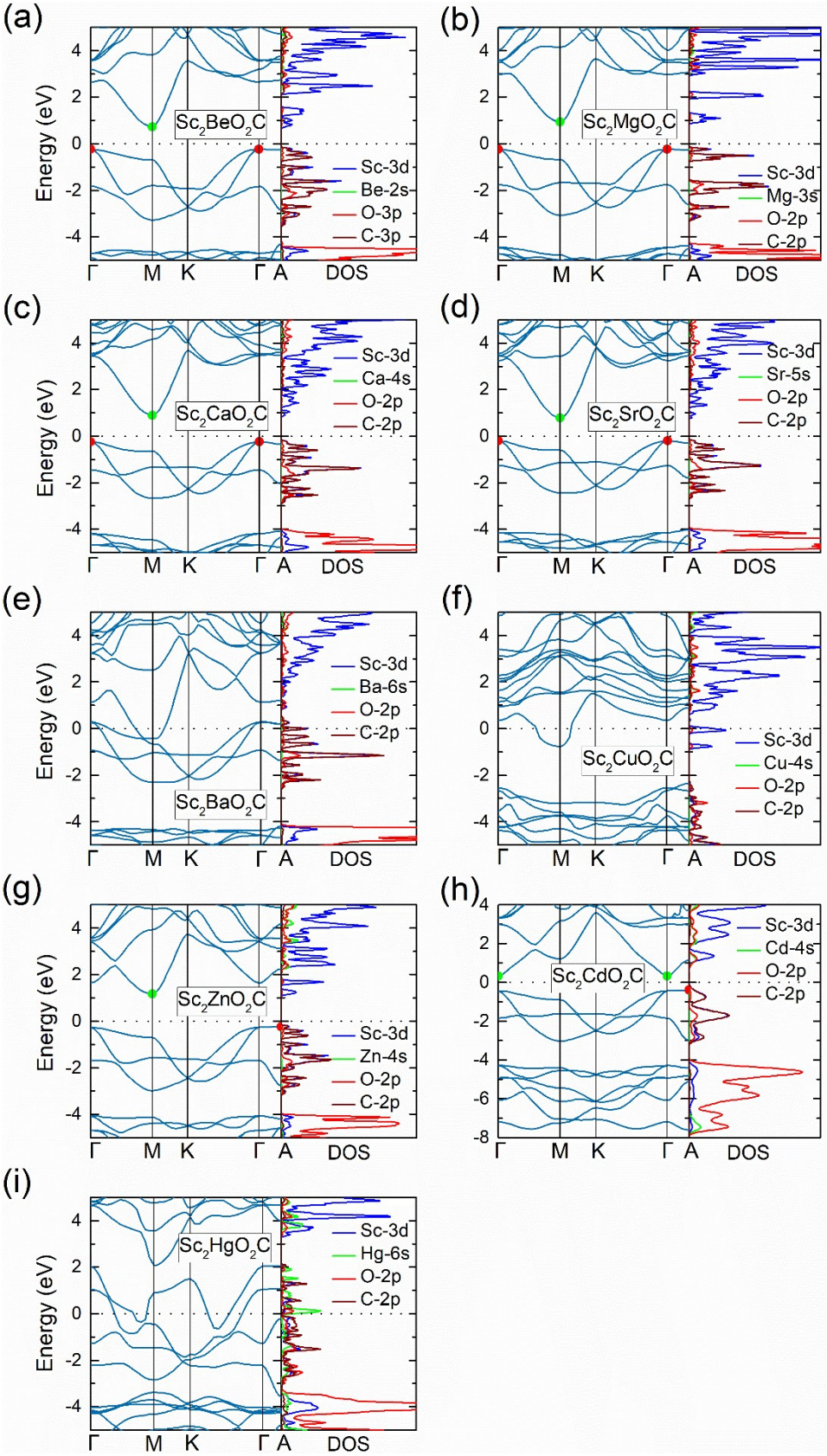

Figure S3. The band structures and the projected density of state (PDOS) of the nine Sc_2AO_2C: (a) Sc_2BeO_2C, (b) Sc_2MgO_2C, (c) Sc_2CaO_2C, (d) Sc_2SrO_2C, (e) Sc_2BaO_2C, (f) Sc_2CuO_2C, (g) Sc_2ZnO_2C, (h) Sc_2CdO_2C and (i) Sc_2HgO_2C. For the semiconductors, the

valence band maximum and conduction band minimum are marked in red and green circles. The black dot line indicates the Fermi level.

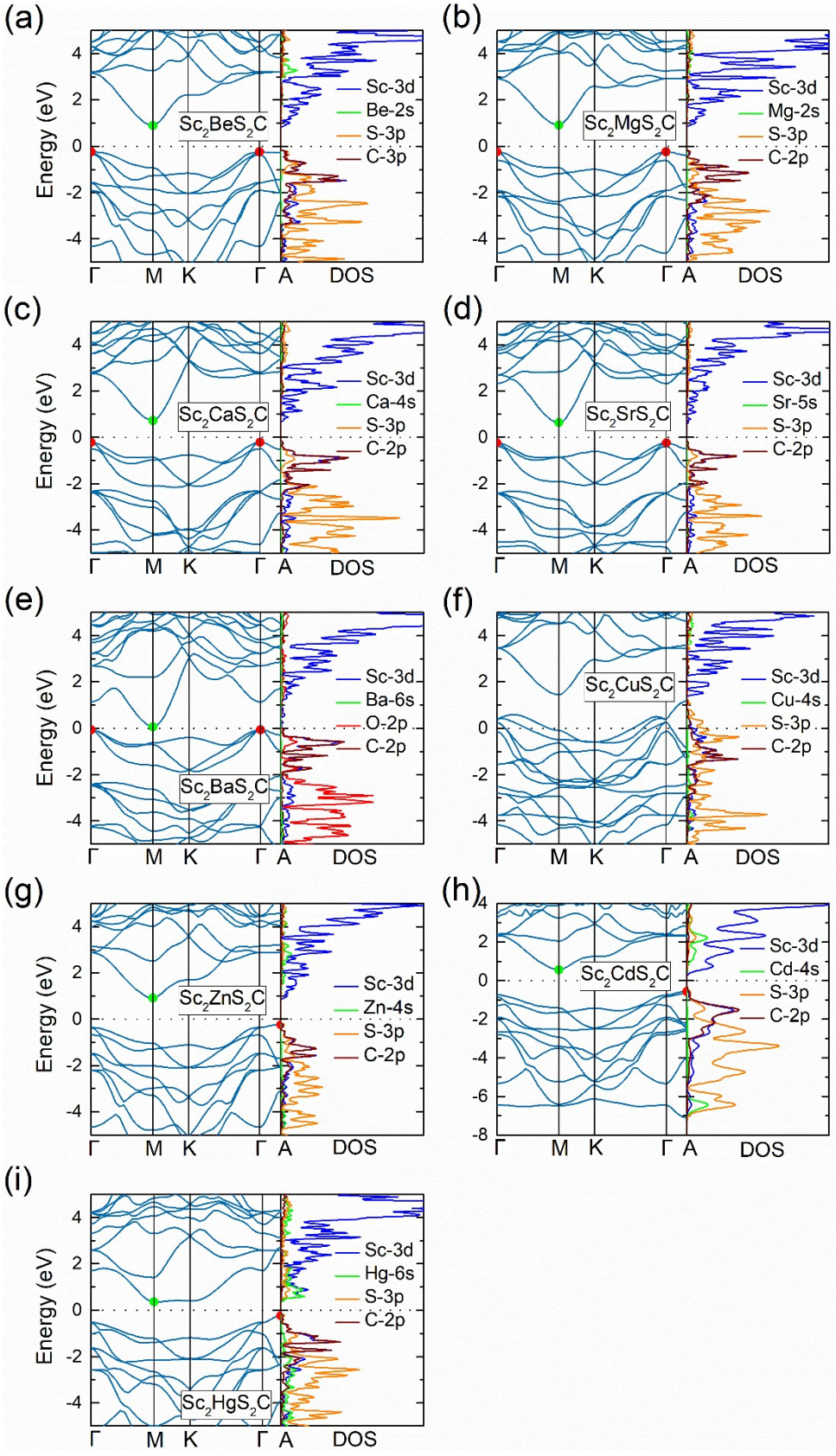

Figure S4. The band structures and the projected density of state (PDOS) of the nine Sc_2AS_2C: (a) Sc_2BeS_2C, (b) Sc_2MgS_2C, (c) Sc_2CaS_2C, (d) Sc_2SrS_2C, (e) Sc_2BaS_2C, (f) Sc_2CuS_2C, (g) Sc_2ZnS_2C, (h) Sc_2CdS_2C and (i) Sc_2HgS_2C. For the semiconductors, the valence band maximum and conduction band minimum are marked in red and green circles. The black dot line indicates the Fermi level.

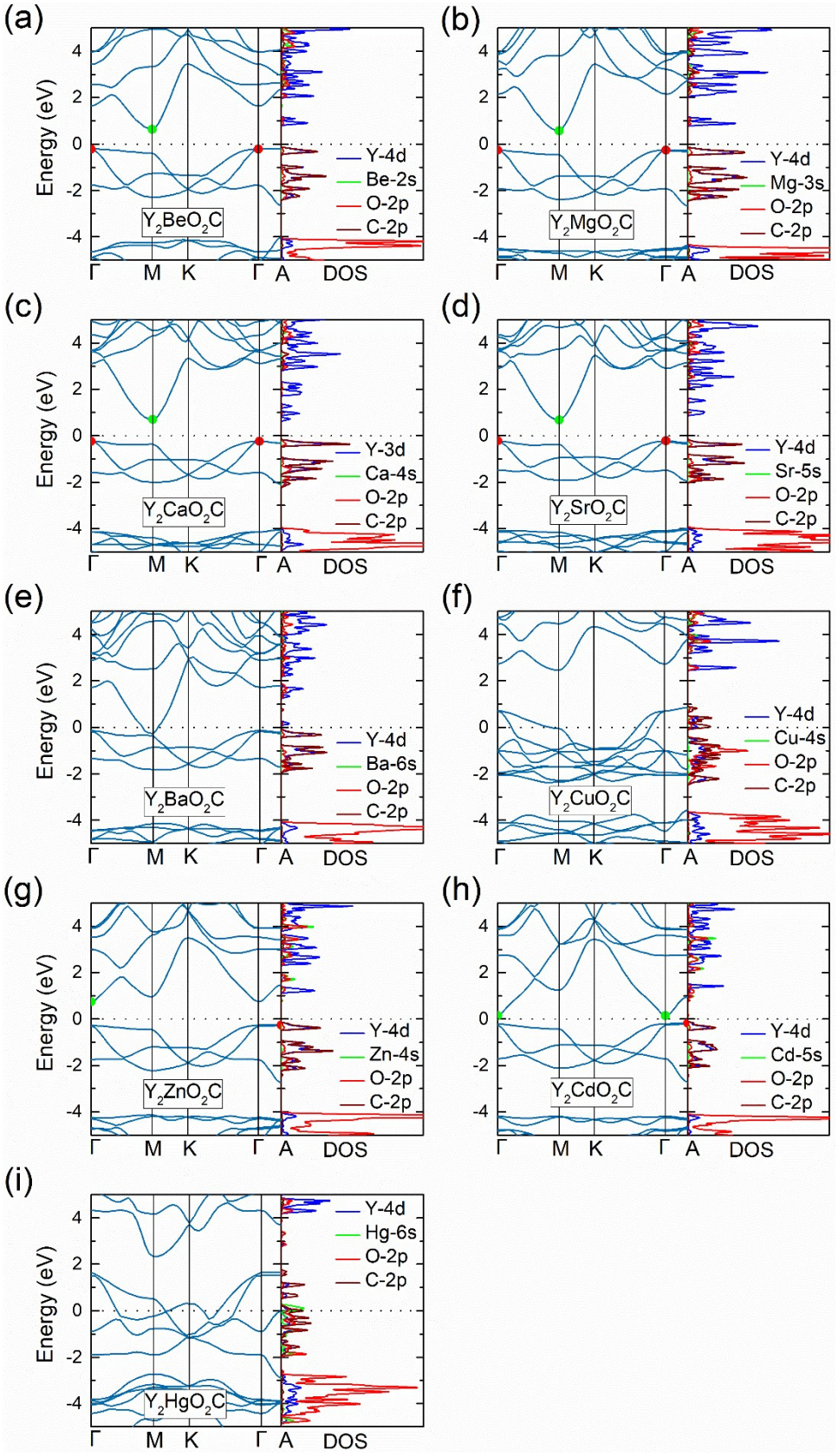

Figure S5. The band structures and the projected density of state (PDOS) of the nine Y_2AO_2C: (a) Y_2BeO_2C, (b) Y_2MgO_2C, (c) Y_2CaO_2C, (d) Y_2SrO_2C, (e) Y_2BaO_2C, (f) Y_2CuO_2C, (g) Y_2ZnO_2C, (h) Y_2CdO_2C and (i) Y_2HgO_2C. For the semiconductors, the valence band

maximum and conduction band minimum are marked in red and green circles. The black dot line indicates the Fermi level.

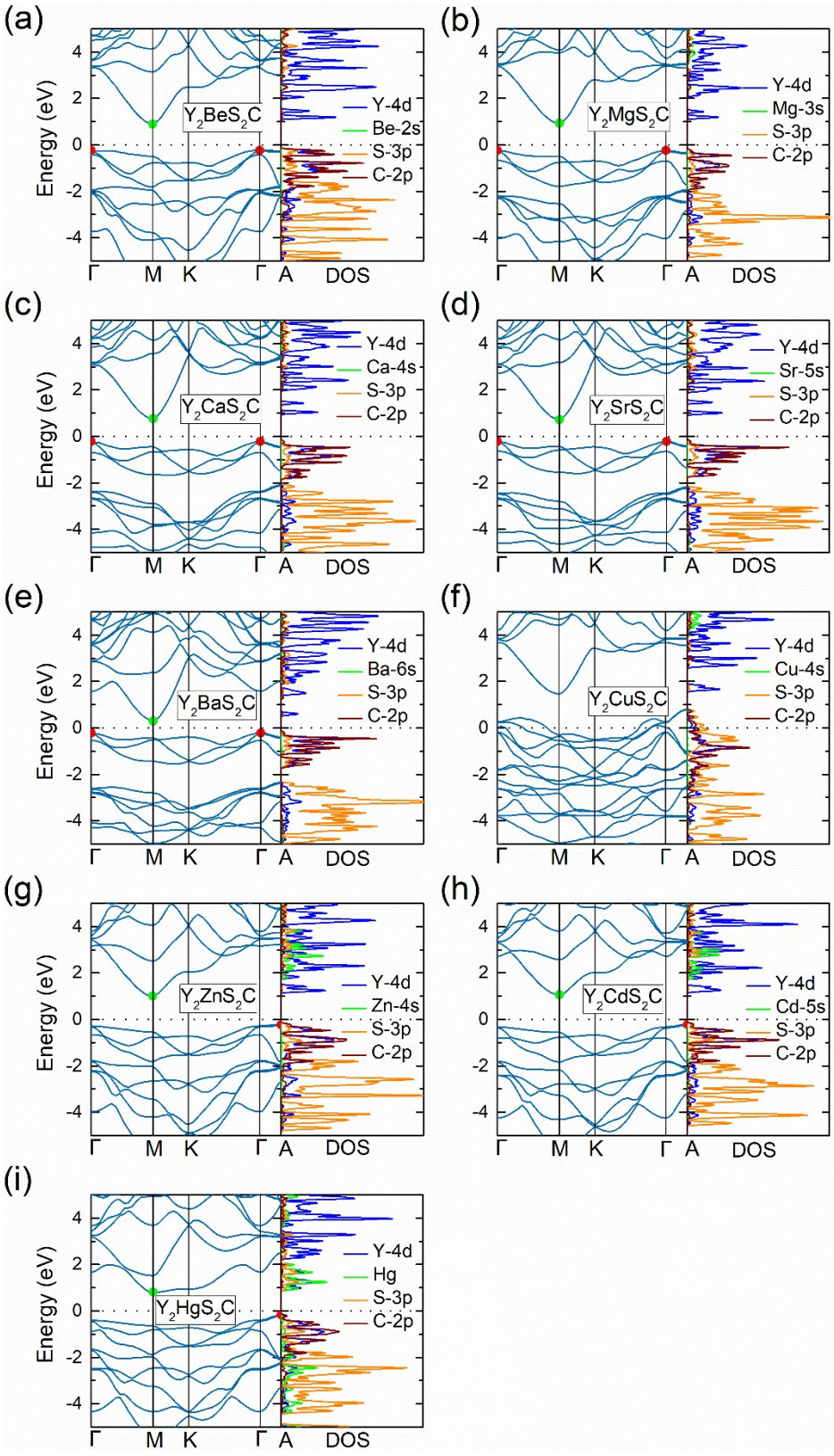

Figure S6. The band structures and the projected density of state (PDOS) of the nine Y_2AS_2C: (a) Y_2BeS_2C, (b) Y_2MgS_2C, (c) Y_2CaS_2C, (d) Y_2SrS_2C, (e) Y_2BaS_2C, (f) Y_2CuS_2C, (g) Y_2ZnS_2C, (h) Y_2CdS_2C and (i) Y_2HgS_2C. For the semiconductors, the valence band maximum and conduction band minimum are marked in red and green circles. The black dot line indicates the Fermi level.

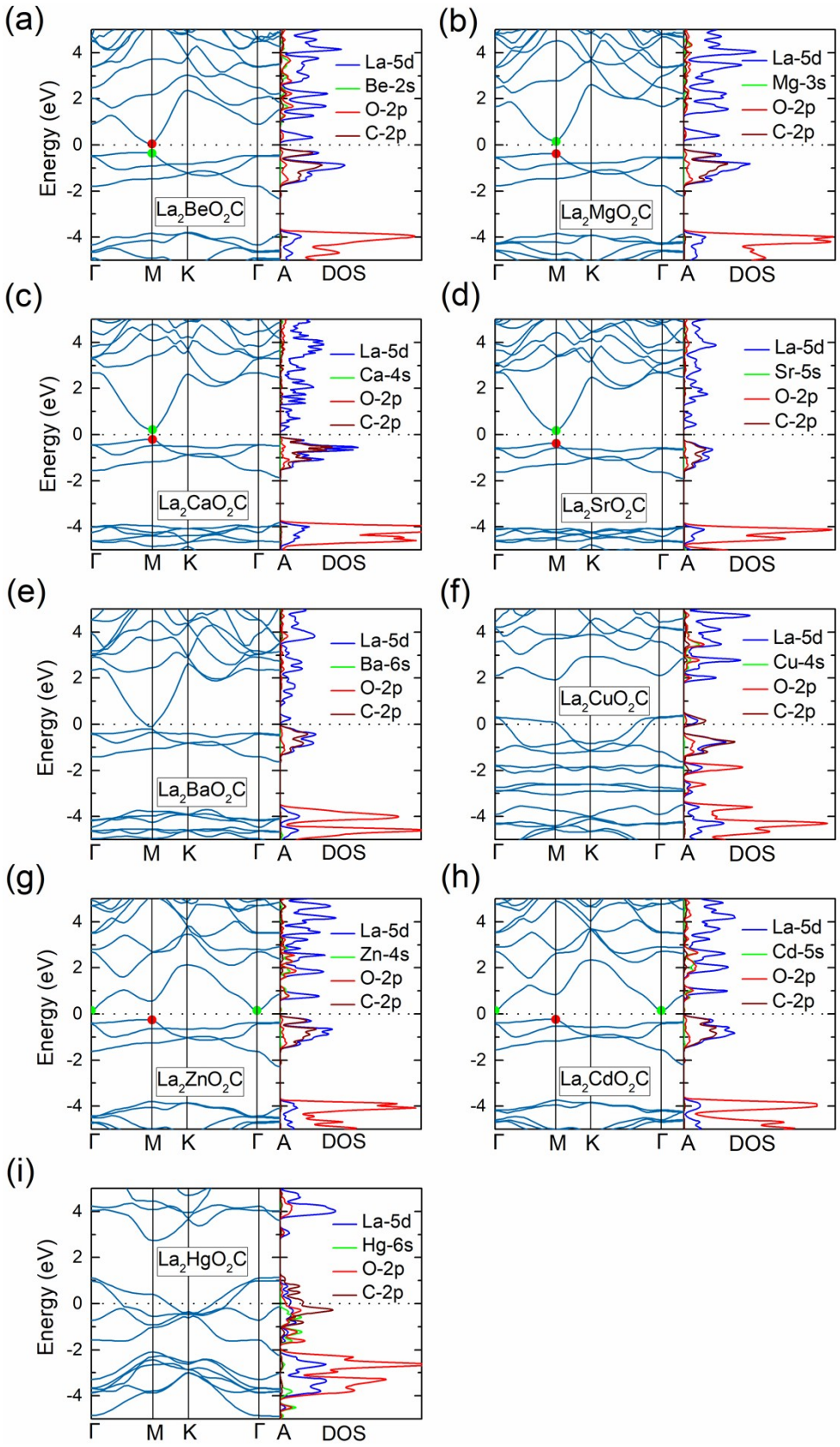

Figure S7. The band structures and the projected density of state (PDOS) of the nine $LaAO_2C$: (a) La_2BeO_2C, (b) La_2MgO_2C, (c) La_2CaO_2C, (d) La_2SrO_2C, (e) La_2BaO_2C, (f) La_2CuO_2C, (g) La_2ZnO_2C, (h) La_2CdO_2C and (i) La_2HgO_2C. For the semiconductors, the valence band

maximum and conduction band minimum are marked in red and green circles. The black dot line indicates the Fermi level.

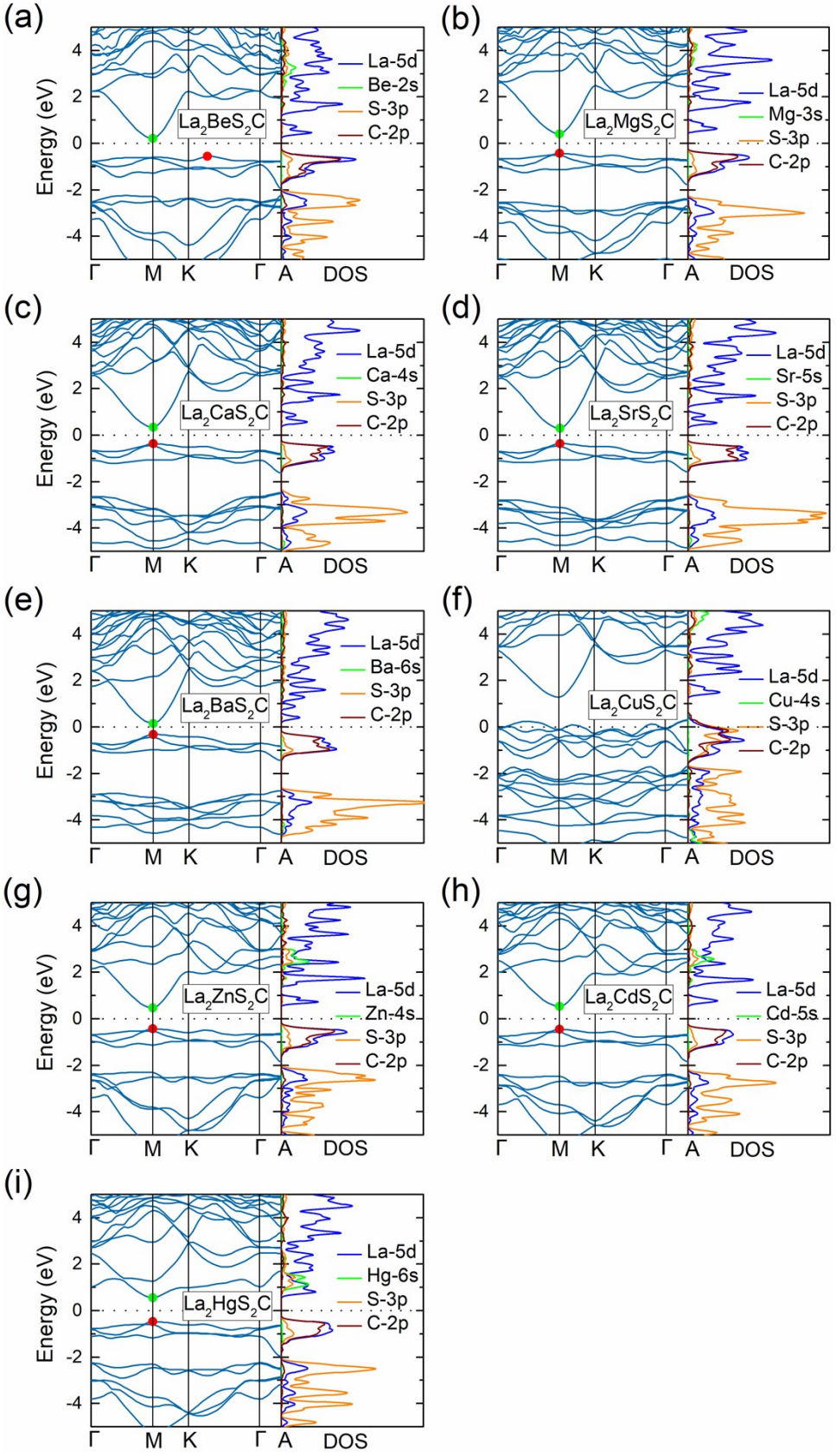

Figure S8. The band structures and the projected density of state (PDOS) of the nine $LaAS_2C$: (a) La_2BeS_2C, (b) La_2MgS_2C, (c) La_2CaS_2C, (d) La_2SrS_2C, (e) La_2BaS_2C, (f) La_2CuS_2C, (g) La_2ZnS_2C, (h) La_2CdS_2C and (i) La_2HgS_2C. For the semiconductors, the valence band maximum and conduction band minimum are marked in red and green circles. The black dot line indicates the Fermi level.

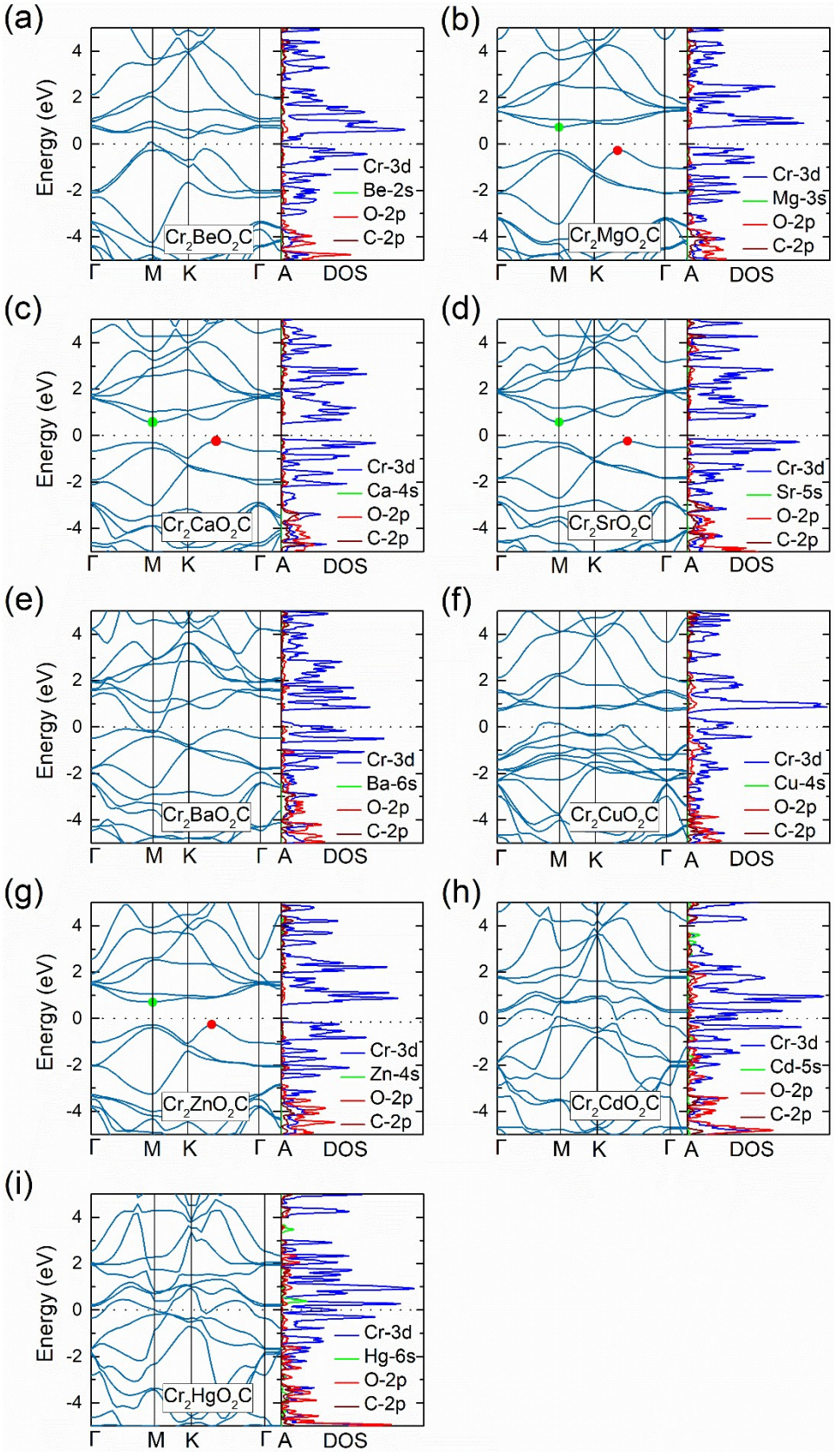

Figure S9. The band structures and the projected density of state (PDOS) of the nine Cr_2AO_2C: (a) Cr_2BeO_2C, (b) Cr_2MgO_2C, (c) Cr_2CaO_2C, (d) Cr_2SrO_2C, (e) Cr_2BaO_2C, (f) Cr_2CuO_2C, (g) Cr_2ZnO_2C, (h) Cr_2CdO_2C and (i) Cr_2HgO_2C. For the semiconductors, the

valence band maximum and conduction band minimum are marked in red and green circles. The black dot line indicates the Fermi level.

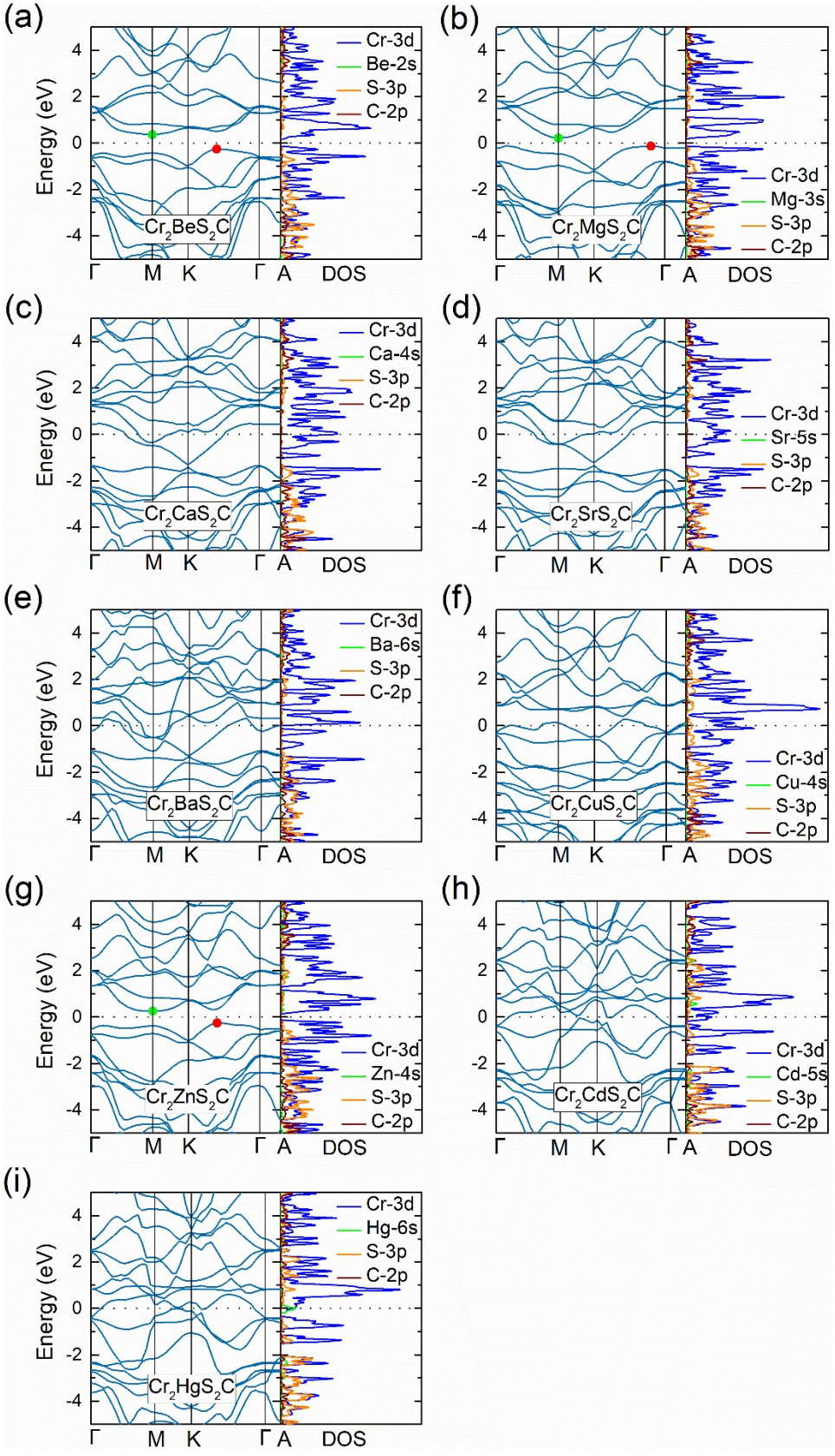

Figure S10. The band structures and the projected density of state (PDOS) of the nine Cr_2AS_2C: (a) Cr_2BeS_2C, (b) Cr_2MgS_2C, (c) Cr_2CaS_2C, (d) Cr_2SrS_2C, (e) Cr_2BaS_2C, (f)

Cr_2CuS_2C, (g) Cr_2ZnS_2C, (h) Cr_2CdS_2C and (i) Cr_2HgS_2C. For the semiconductors, the valence band maximum and conduction band minimum are marked in red and green circles. The black dot line indicates the Fermi level.

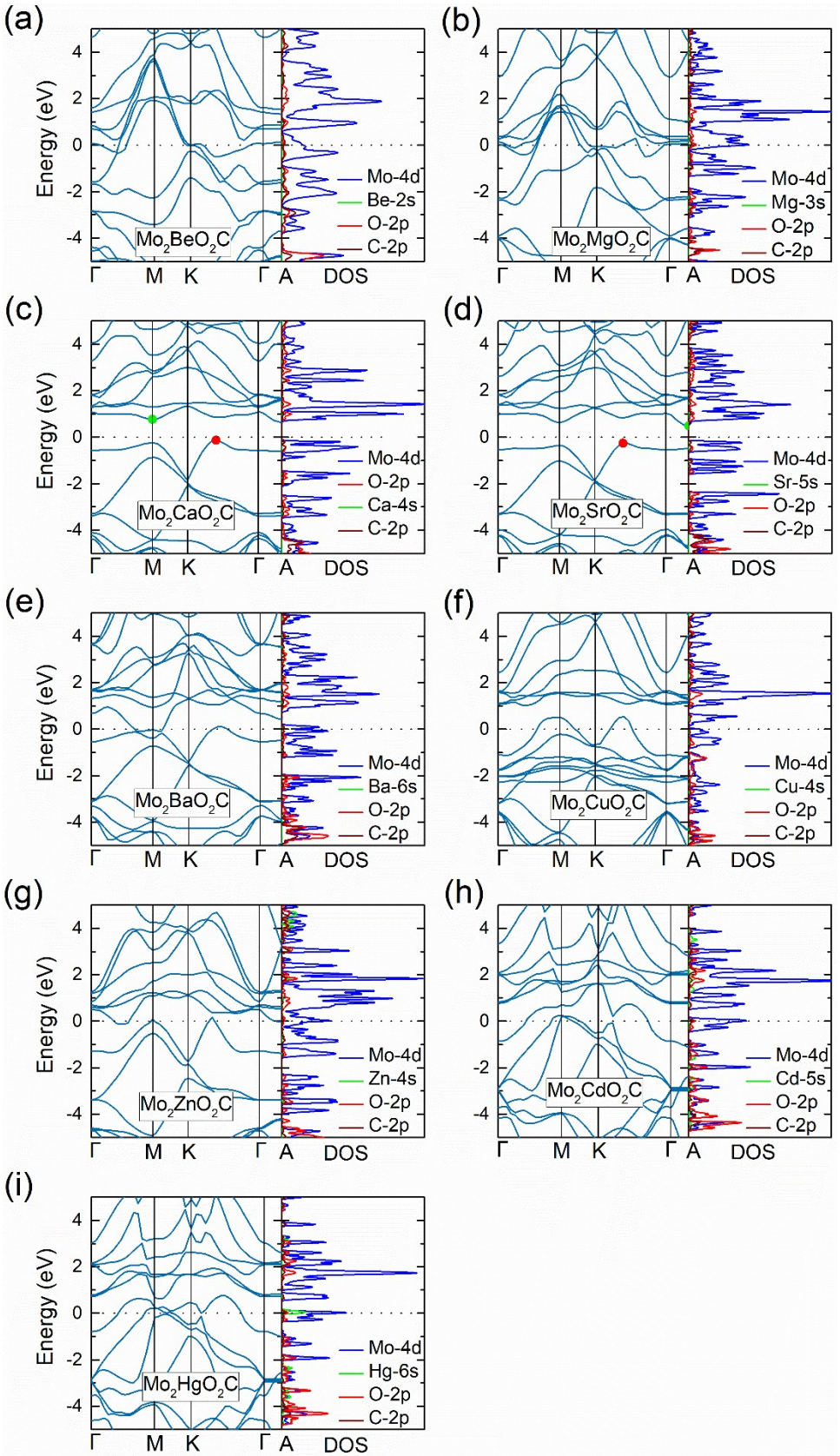

Figure S11. The band structures and the projected density of state (PDOS) of the nine Mo_2AO_2C: (a) Mo_2BeO_2C, (b) Mo_2MgO_2C, (c) Mo_2CaO_2C, (d) Mo_2SrO_2C, (e) Mo_2BaO_2C, (f) Mo_2CuO_2C, (g) Mo_2ZnO_2C, (h) Mo_2CdO_2C and (i) Mo_2HgO_2C. For the semiconductors, the valence band maximum and conduction band minimum are marked in red and green circles. The black dot line indicates the Fermi level.

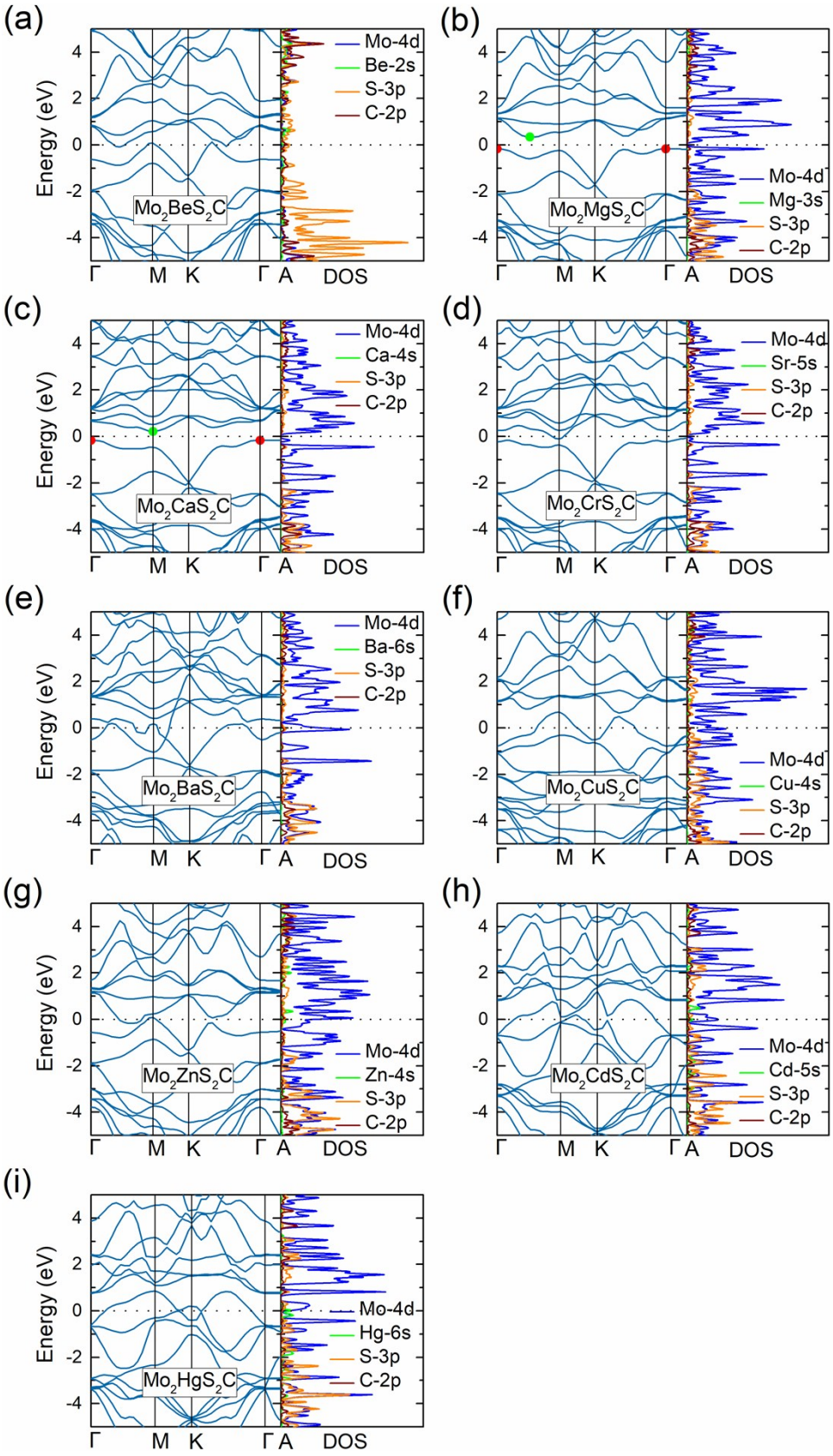

Figure S12. The band structures and the projected density of state (PDOS) of the nine Mo_2AS_2C: (a) Mo_2BeS_2C, (b) Mo_2MgS_2C, (c) Mo_2CaS_2C, (d) Mo_2SrS_2C, (e) Mo_2BaS_2C, (f) Mo_2CuS_2C, (g) Mo_2ZnS_2C, (h) Mo_2CdS_2C and (i) Mo_2HgS_2C. For the semiconductors, the

valence band maximum and conduction band minimum are marked in red and green circles. The black dot line indicates the Fermi level.

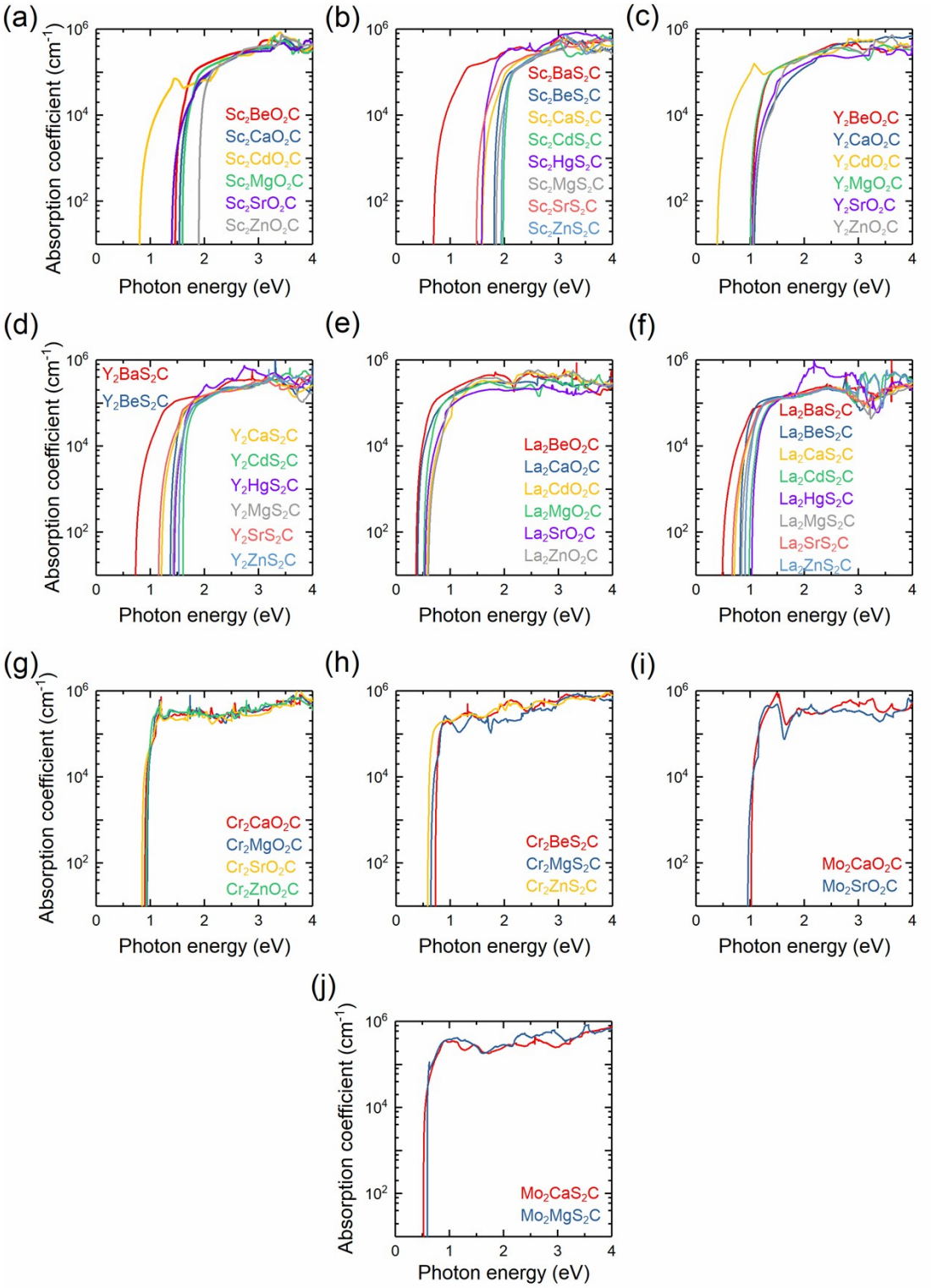

Figure S13. Optical absorption spectra of (a) Sc-based oxycarbide MAOX, (b) Sc-based sulcarbide MAOX, (c) Y-based oxycarbide MAOX, (d) Y-based sulcarbide MAOX, (e) La-based oxycarbide MAOX, (f) La-based sulcarbide MAOX, (g) Cr-based oxycarbide MAOX, (h) Cr-based sulcarbide MAOX, (i) Mo-based oxycarbide MAOX and (j) Mo-based sulcarbide MAOX.

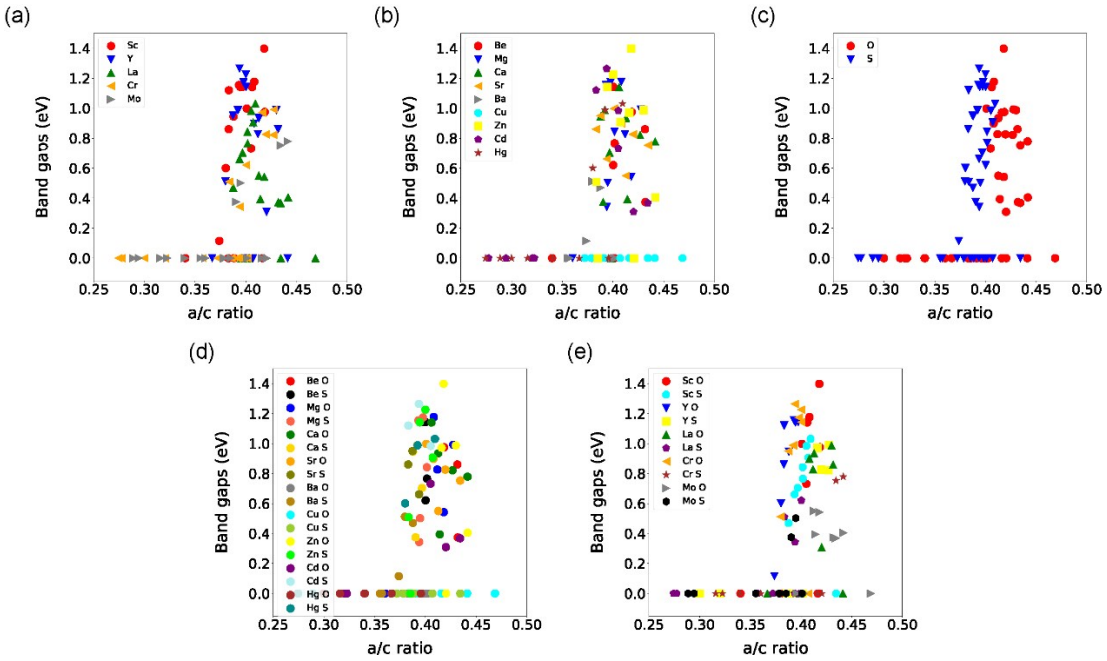

Figure S14. Fundamental bandgap dispersion for 90 MAOX phases classified by (a) M, (b) A, (c) O, (d) AO and (e) MO. The compounds in the same group are in the same color.

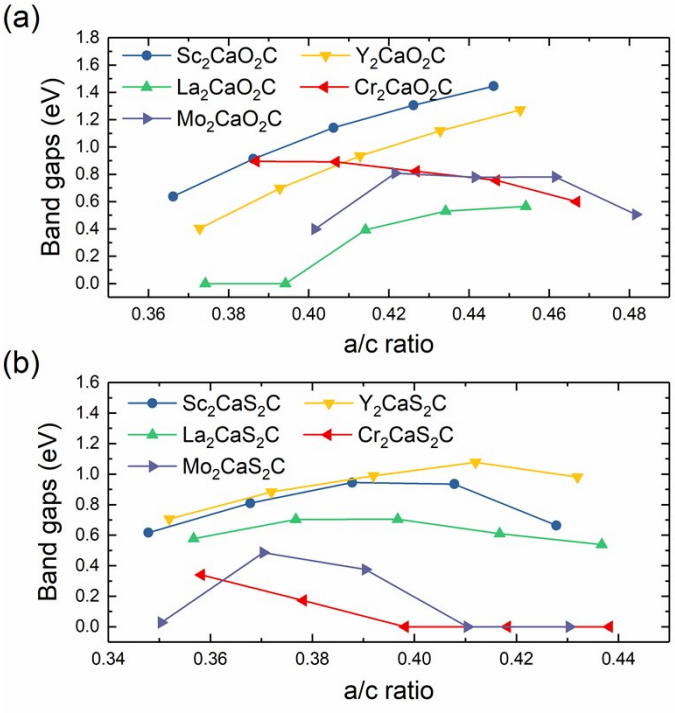

Figure S15. The fundamental bandgaps as the function of the a/c ratios for (a) five oxycarbide and (b) five sulcarbide MAOX semiconductors.

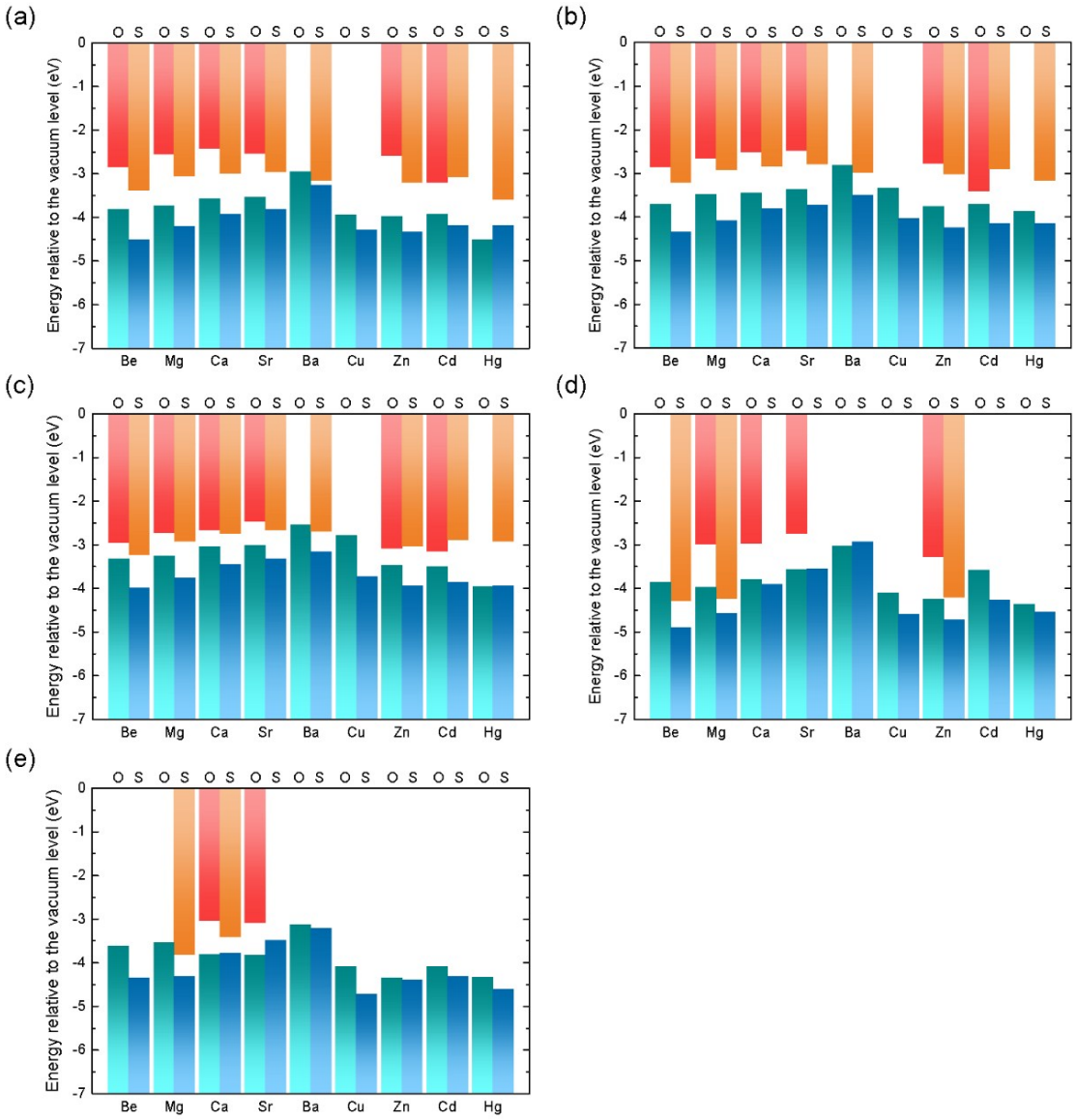

Figure S16. Band alignment for ninety MAOX: (a) Sc-based, (b) Y-based, (c) La-based, (d) Cr-based and (e) Mo-based MAOX with respect to vacuum level at 0 eV.

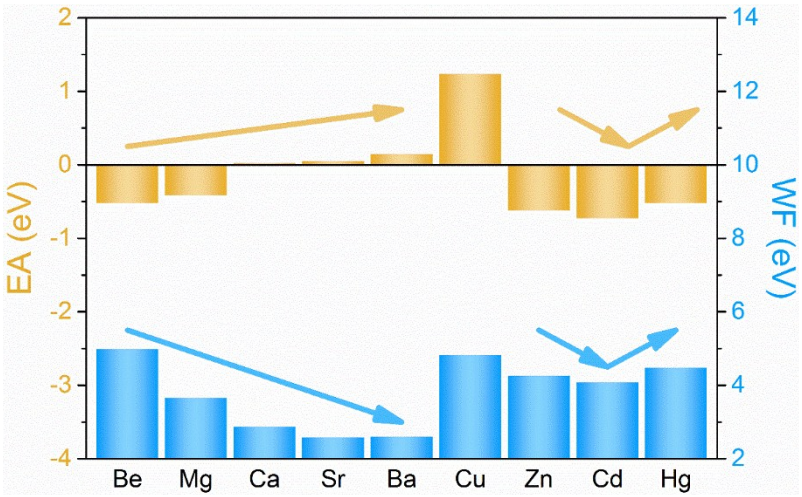

Figure S17. Electron affinities (EAs) and work functions (WFs) according to A.

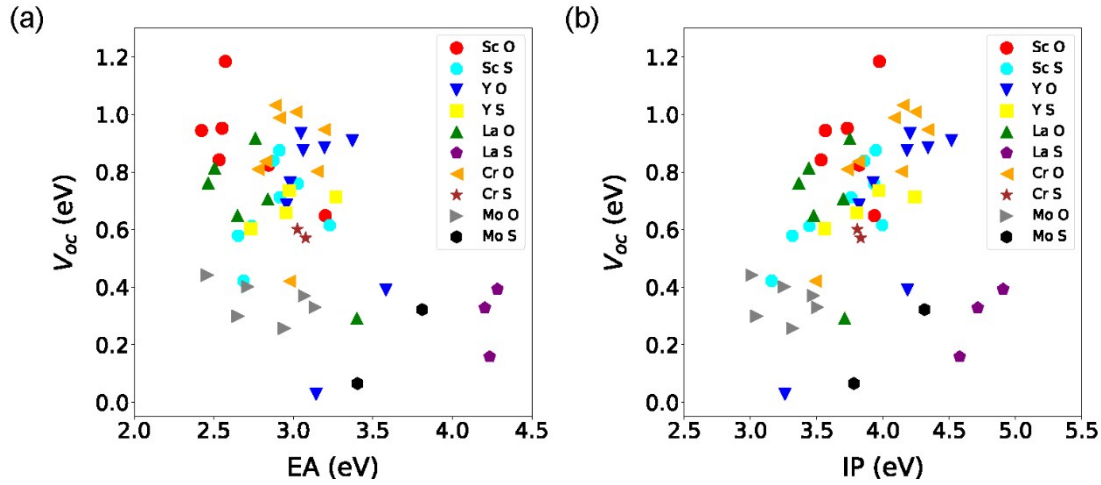

Figure S18. V_{oc} versus (a) electron affinity (EA) and (b) ionization potential (IP) of MAOX semiconductors.

Table S1. Formation energy (ΔG_f) of MAOX phase and the competing phase in the estimation, where the space groups of M/A oxides/sulfides/carbides are shown in the parentheses

MAOX	Competing phase	ΔG_f(eV)
Sc_2BaO_2C	Sc_2C ($P\bar{3}m1$), BaO ($Fm\bar{3}m$), O_2	-4.975
Sc_2BaS_2C	Sc_2S_3 (Fddd), BaS ($Fm\bar{3}m$), BaC_2 (C2/c), Sc	-0.707
Sc_2BeO_2C	Sc_2C ($P\bar{3}m1$), BeO ($P6_3mc$), O_2	-3.752
Sc_2BeS_2C	Sc_2C ($P\bar{3}m1$), BeS ($F\bar{4}3m$), S	-2.610
Sc_2CaO_2C	Sc_2O_3 (Ia3), Sc, CaO ($Fm\bar{3}m$), CaC_2 (I4/mmm)	-1.483
Sc_2CaS_2C	Sc_2S_3 (Fddd), CaS ($Fm\bar{3}m$), CaC_2 (I4/mmm), Sc	-1.826
Sc_2CdO_2C	Sc_2O_3 (Ia3), CdC ($Fm\bar{3}m$), Sc	-1.682
Sc_2CdS_2C	Sc_2S_3 (Fddd), CdC ($Fm\bar{3}m$), Sc	-3.311
Sc_2CuO_2C	Sc_2C ($P\bar{3}m1$), CuO ($P4_2/mmc$), O_2	-6.226
Sc_2CuS_2C	Sc_2C ($P\bar{3}m1$), CuS (Cmcm), S	-3.111
Sc_2HgO_2C	Sc_2C ($P\bar{3}m1$), HgO (Pnma), O_2	-6.373
Sc_2HgS_2C	Sc_2C ($P\bar{3}m1$), HgS ($F\bar{4}3m$), S	-2.618

Sc_2MgO_2C	Sc_2C ($P\bar{3}m1$), MgO ($Fm\bar{3}m$), O_2	-6.081
Sc_2MgS_2C	Sc_2C ($P\bar{3}m1$), MgS ($Fm\bar{3}m$), S	-3.646
Sc_2SrO_2C	Sc_2O_3 (Ia3), SrO ($Fm\bar{3}m$), SrC_2 (C2/c), Sc	-0.481
Sc_2SrS_2C	Sc_2S_3 (Fddd), SrS ($Fm\bar{3}m$), SrC_2 (C2/c), Sc	-1.275
Sc_2ZnO_2C	Sc_2C ($P\bar{3}m1$), ZnO ($P6_3mc$), O_2	-5.875
Sc_2ZnS_2C	Sc_2C ($P\bar{3}m1$), ZnS ($F\bar{4}3m$), S	-2.964
Y_2BaO_2C	Y_2O_3 (Ia3), BaO ($Fm\bar{3}m$), BaC_2 (C2/c), Y	-0.041
Y_2BaS_2C	Y_2S_3 ($P2_1/m$), BaS ($Fm\bar{3}m$), BaC_2 (C2/c), Y	-1.171
Y_2BeO_2C	Y_2C ($R\bar{3}m$), BeO ($P6_3mc$), O_2	-2.323
Y_2BeS_2C	Y_2C ($R\bar{3}m$), BeS ($F\bar{4}3m$), S	-2.653
Y_2CaO_2C	Y_2O_3 (Ia3), CaO ($Fm\bar{3}m$), CaC_2 (I4/mmm), Y	-0.911
Y_2CaS_2C	Y_2S_3 ($P2_1/m$), CaS ($Fm\bar{3}m$), CaC_2 (I4/mmm), Y	-1.934
Y_2CdO_2C	Y_2O_3 (Ia3), CdC ($Fm\bar{3}m$), Y	-1.148
Y_2CdS_2C	Y_2S_3 ($P2_1/m$), CdC ($Fm\bar{3}m$), Y	-3.019
Y_2CuO_2C	Y_2C ($R\bar{3}m$), CuO ($P4_2/mmc$), O_2	-5.980
Y_2CuS_2C	Y_2C ($R\bar{3}m$), CuS (Cmcm), S	-3.468
Y_2HgO_2C	Y_2C ($R\bar{3}m$), HgO (Pnma), O_2	-6.323
Y_2HgS_2C	Y_2C ($R\bar{3}m$), HgS ($F\bar{4}3m$), S	-3.406
Y_2MgO_2C	Y_2C ($R\bar{3}m$), MgO ($Fm\bar{3}m$), O_2	-4.963
Y_2MgS_2C	Y_2C ($R\bar{3}m$), MgS ($Fm\bar{3}m$), S	-4.106
Y_2SrO_2C	Y_2O_3 (Ia3), SrO ($Fm\bar{3}m$), SrC_2 (C2/c), Y	-0.210
Y_2SrS_2C	Y_2S_3 ($P2_1/m$), SrS ($Fm\bar{3}m$), SrC_2 (C2/c), Y	-1.596
Y_2ZnO_2C	Y_2C ($R\bar{3}m$), ZnO ($P6_3mc$), O_2	-5.189
Y_2ZnS_2C	Y_2C ($R\bar{3}m$), ZnS ($F\bar{4}3m$), S	-3.358
La_2BaO_2C	LaC_2 (I4/mmm), BaO ($Fm\bar{3}m$), La, O_2	-4.771
La_2BaS_2C	La_2S_3 (Pnma), BaS ($Fm\bar{3}m$), BaC_2 (C2/c), La	-0.655
La_2BeO_2C	LaC_2 (I4/mmm), BeO ($P6_3mc$), La, O2	-0.888
La_2BeS_2C	LaC_2 (I4/mmm), BeS ($F\bar{4}3m$), La, S	-2.115
La_2CaO_2C	La_2O_3 ($P\bar{3}m1$), La, CaO ($Fm\bar{3}m$), CaC_2 (I4/mmm)	-1.273
La_2CaS_2C	La_2S_3 (Pnma), CaS ($Fm\bar{3}m$), CaC_2 (I4/mmm), La	-0.909
La_2CdO_2C	La_2O_3 ($P\bar{3}m1$), CdC ($Fm\bar{3}m$), La	-0.371
La_2CdS_2C	La_2S_3 (Pnma), CdC ($Fm\bar{3}m$), La	-2.061
La_2CuO_2C	LaC_2 (I4/mmm), CuO ($P4_2/mmc$), La, O2	-5.308
La_2CuS_2C	LaC_2 (I4/mmm), CuS (Cmcm), La, S	-3.298
La_2HgO_2C	La_2C (I4/mmm), HgO (Pnma), O_2	-1.842
La_2HgS_2C	LaC_2 (I4/mmm), HgS ($F\bar{4}3m$), La, S	-3.486
La_2MgO_2C	LaC_2 (I4/mmm), MgO ($Fm\bar{3}m$), La, O_2	-3.961
La_2MgS_2C	LaC_2 (I4/mmm), MgS ($Fm\bar{3}m$), La, S	-3.915
La_2SrO_2C	LaC_2 (I4/mmm), SrO ($Fm\bar{3}m$), La, O_2	-4.758
La_2SrS_2C	La_2S_3 (Pnma), SrS ($Fm\bar{3}m$), SrC_2 (C2/c), La	-0.781
La_2ZnO_2C	LaC_2 (I4/mmm), ZnO ($P6_3mc$), La, O_2	-4.266
La_2ZnS_2C	LaC_2 (I4/mmm), ZnS ($F\bar{4}3m$), La, S	-3.193
Cr_2BaO_2C	Cr_2O_3 ($R\bar{3}c$), BaC_2 (C2/c), Cr, Ba	-2.598
Cr_2BaS_2C	Cr_2S_3 (R3), BaC_2 (C2/c), Cr, Ba	-3.323

Cr_2BeO_2C	Cr_3C_2 (Pnma), BeO ($P6_3mc$), Cr, O_2	-0.164
Cr_2BeS_2C	Cr_2S_3 (R3), Cr_3C_2 (Pnma), Be, S	-0.447
Cr_2CaO_2C	Cr_2O_3 ($R\bar{3}c$), Cr, CaO ($Fm\bar{3}m$), CaC_2 (I4/mmm)	-0.134
Cr_2CaS_2C	Cr_2S_3 (R3), CaS ($Fm\bar{3}m$), Cr, S	-3.336
Cr_2CdO_2C	Cr_3C_2 (Pnma), CdO ($Fm\bar{3}m$), Cr, O_2	-1.911
Cr_2CdS_2C	Cr_2S_3 (R3), Cr_3C_2 (Pnma), Cd, S	-0.430
Cr_2CuO_2C	Cr_3C_2 (Pnma), CuO ($P4_2/mmc$), Cr, O_2	-2.007
Cr_2CuS_2C	Cr_3C_2 (Pnma), CuS (Cmcm), Cr, S	-0.148
Cr_2HgO_2C	Cr_2S_3 (R3), Cr_3C_2 (Pnma), HgO (Pnma), O_2	-1.008
Cr_2HgS_2C	C_2S_3 (R3), Cr_3C_2, (Pnma) HgS ($F\bar{4}3m$), S	-0.117
Cr_2MgO_2C	Cr_3C_2 (Pnma), MgO ($Fm\bar{3}m$), Cr, O_2	-1.696
Cr_2MgS_2C	Cr_2S_3 (R3), Cr_3C_2 (Pnma), Mg, S	-1.415
Cr_2SrO_2C	Cr_3C_2 (Pnma), SrO ($Fm\bar{3}m$), Cr, O_2	-6.279
Cr_2SrS_2C	Cr_3C_2 (Pnma), SrS ($Fm\bar{3}m$), Cr, S	-2.518
Cr_2ZnO_2C	Cr_3C_2 (Pnma), ZnO ($P6_3mc$), Cr, O_2	-1.413
Cr_2ZnS_2C	Cr_2S_3 (R3), Cr_3C_2 (Pnma), Zn, S	-0.121
Mo_2BaO_2C	MoC ($P\bar{6}m2$), BaO ($Fm\bar{3}m$), Mo, O_2	-0.999
Mo_2BaS_2C	MoS_2 ($P6_3mmc$), BaC_2 (C2/c), Mo, Ba	-0.481
Mo_2BeO_2C	MoC ($P\bar{6}m2$), BeO ($P6_3mc$), Mo, O_2	-0.160
Mo_2BeS_2C	Mo_2C (Pbcn), Be, S	-1.065
Mo_2CaO_2C	MoO_2 ($P4_2/mnm$), Mo, CaO ($Fm\bar{3}m$), CaC_2 (I4/mmm)	-0.883
Mo_2CaS_2C	MoS_2 ($P6_3mmc$), CaC_2 (I4/mmm), Mo, Ca	-1.320
Mo_2CdO_2C	MoC ($P\bar{6}m2$), CdO ($Fm\bar{3}m$), Mo, O_2	-2.647
Mo_2CdS_2C	MoC ($P\bar{6}m2$), CdS ($P6_3mc$), Mo, S	-0.556
Mo_2CuO_2C	MoC ($P\bar{6}m2$), CuO ($P4_2/mmc$), Mo, O_2	-2.310
Mo_2CuS_2C	MoC ($P\bar{6}m2$), CuS (Cmcm), Mo, S	-1.071
Mo_2HgO_2C	MoO_2 ($P4_2/mnm$), MoC ($P\bar{6}m2$), HgO (Pnma), Mo	-0.930
Mo_2HgS_2C	MoS_2 ($P6_3mmc$), MoC ($P\bar{6}m2$), HgS ($F\bar{4}3m$), Mo	-0.092
Mo_2MgO_2C	MoO_2 ($P4_2/mnm$), MoC ($P\bar{6}m2$), MgO ($Fm\bar{3}m$), Mo	-1.372
Mo_2MgS_2C	MoC ($P\bar{6}m2$), MgS ($Fm\bar{3}m$), Mo, S	-0.152
Mo_2SrO_2C	MoO_2 ($P4_2/mnm$), SrO ($Fm\bar{3}m$), SrC_2 (C2/c), Mo	-0.048
Mo_2SrS_2C	MoS_2 ($P6_3mmc$), SrC_2 (C2/c), Mo, Sr	-0.730
Mo_2ZnO_2C	MoC ($P\bar{6}m2$), ZnO ($P6_3mc$), Mo, O_2	-1.446
Mo_2ZnS_2C	MoC ($P\bar{6}m2$), ZnS ($F\bar{4}3m$), Mo, S	-0.044

Table S2. The lattice parameters given in Å, fundamental indirect and direct bandgaps (E_{ind} and E_{dir}) given in eV, open-circuit voltage (V_{oc}) given in eV and spectroscopic limited maximum efficiencies (SLMEs) given in % at 0.2 μm of M_2AO_2C, where M = Sc, Y, Cr, Mo and La, and A = Be, Mg, Ca, Sr, Ba, Cu, Zn, Cd, and Hg, based on the HSE06 calculations. In. Semi. and Di. Semi. stand for the indirect and direct semiconductor.

MAOX	*a*	*c*	E_{ind}	E_{dir}	Type	V_{oc}	SLMEs
Sc_2BaO_2C	3.344	8.737	0	0	Metal	-	-

Sc_2BaS_2C	3.691	9.874	0.115	0.688	In. Semi.	0.028	0.444
Sc_2BeO_2C	3.103	7.413	0.975	1.424	In. Semi.	0.824	17.873
Sc_2BeS_2C	3.410	8.584	1.144	1.820	In. Semi.	0.909	13.146
Sc_2CaO_2C	3.283	8.083	1.141	1.546	In. Semi.	0.944	17.493
Sc_2CaS_2C	3.601	9.285	0.945	1.597	In. Semi.	0.763	12.487
Sc_2CdO_2C	3.287	8.112	0.732	0.780	In. Semi.	0.648	21.056
Sc_2CdS_2C	3.567	9.306	1.120	1.976	In. Semi.	0.875	10.226
Sc_2CuO_2C	3.208	7.702	0	0	Metal	-	-
Sc_2CuS_2C	3.450	8.881	0	0	Metal	-	-
Sc_2HgO_2C	3.187	9.365	0	0	Metal	-	-
Sc_2HgS_2C	3.570	9.391	0.601	1.584	In. Semi.	0.390	6.885
Sc_2MgO_2C	3.173	7.771	1.177	1.619	In. Semi.	0.952	17.711
Sc_2MgS_2C	3.519	8.950	1.154	1.855	In. Semi.	0.934	12.010
Sc_2SrO_2C	3.340	8.331	0.998	1.397	In. Semi.	0.842	16.300
Sc_2SrS_2C	3.655	9.542	0.860	1.484	In. Semi.	0.685	12.865
Sc_2ZnO_2C	3.213	7.686	1.398	1.867	In. Semi.	1.184	16.007
Sc_2ZnS_2C	3.505	8.884	1.142	1.954	In. Semi.	0.885	10.930
Y_2BaO_2C	3.592	9.003	0	0	Metal	-	-
Y_2BaS_2C	3.900	10.268	0.512	0.722	In. Semi.	0.421	15.020
Y_2BeO_2C	3.354	7.771	0.860	1.035	In. Semi.	0.706	23.988
Y_2BeS_2C	3.618	9.039	1.143	1.384	In. Semi.	0.947	23.611
Y_2CaO_2C	3.498	8.474	0.935	1.071	In. Semi.	0.813	22.068
Y_2CaS_2C	3.799	9.692	0.988	1.213	In. Semi.	0.837	21.656
Y_2CdO_2C	3.520	8.375	0.309	0.344	In. Semi.	0.291	12.231
Y_2CdS_2C	3.775	9.588	1.264	1.612	In. Semi.	1.032	20.719
Y_2CuO_2C	3.468	7.860	0	0	Metal	-	-
Y_2CuS_2C	3.693	9.074	0	0	Metal	-	-
Y_2HgO_2C	3.508	9.565	0	0	Metal	-	-
Y_2HgS_2C	3.789	9.657	0.988	1.448	In. Semi.	0.802	17.648
Y_2MgO_2C	3.369	8.180	0.827	1.033	In. Semi.	0.649	22.234
Y_2MgS_2C	3.721	9.358	1.173	1.428	In. Semi.	0.988	22.314
Y_2SrO_2C	3.553	8.708	0.898	1.046	In. Semi.	0.761	22.586
Y_2SrS_2C	3.854	9.949	0.950	1.155	In. Semi.	0.809	21.940
Y_2ZnO_2C	3.444	8.008	0.987	1.004	In. Semi.	0.916	26.004
Y_2ZnS_2C	3.707	9.267	1.226	1.533	In. Semi.	1.009	21.807
La_2BaO_2C	3.773	9.375	0	0	Metal	-	-
La_2BaS_2C	4.137	10.672	0.470	-	Di. Semi.	0.422	17.721
La_2BeO_2C	3.565	8.251	0.374	0.390	In. Semi.	0.257	11.614
La_2BeS_2C	3.819	9.507	0.766	0.818	In. Semi.	0.615	25.617
La_2CaO_2C	3.658	8.832	0.394	-	Di. Semi.	0.299	13.582
La_2CaS_2C	4.011	10.110	0.704	-	Di. Semi.	0.612	24.458
La_2CdO_2C	3.745	8.623	0.368	0.518	In. Semi.	0.330	13.069
La_2CdS_2C	3.994	9.854	0.984	-	Di. Semi.	0.839	30.405
La_2CuO_2C	3.753	8.008	0	0	Metal	-	-

La_2CuS_2C	3.967	9.131	0	0	Metal	-	-
La_2HgO_2C	3.857	9.750	0	0	Metal	-	-
La_2HgS_2C	4.030	9.843	1.031	1.029	In. Semi.	0.875	30.884
La_2MgO_2C	3.621	8.660	0.542	0.530	In. Semi.	0.401	18.669
La_2MgS_2C	3.929	9.786	0.842	-	Di. Semi.	0.712	28.092
La_2SrO_2C	3.768	9.129	0.550	-	Di. Semi.	0.442	19.400
La_2SrS_2C	4.071	10.338	0.662	-	Di. Semi.	0.579	23.186
La_2ZnO_2C	3.684	8.340	0.405	0.541	In. Semi.	0.370	15.066
La_2ZnS_2C	3.920	9.626	0.906	-	Di. Semi.	0.759	29.588
Cr_2BaO_2C	3.150	8.164	0	0	Metal	-	-
Cr_2BaS_2C	3.377	9.453	0	0	Metal	-	-
Cr_2BeO_2C	2.830	7.048	0	0	Metal	-	-
Cr_2BeS_2C	3.156	7.885	0.621	0.770	In. Semi.	0.393	17.202
Cr_2CaO_2C	3.112	7.291	0.846	0.898	In. Semi.	0.658	27.726
Cr_2CaS_2C	3.382	8.493	0	0	Metal	-	-
Cr_2CdO_2C	2.911	9.088	0	0	Metal	-	-
Cr_2CdS_2C	3.067	11.061	0	0	Metal	-	-
Cr_2CuO_2C	2.925	7.480	0	0	Metal	-	-
Cr_2CuS_2C	3.137	8.430	0	0	Metal	-	-
Cr_2HgO_2C	2.902	9.675	0	0	Metal	-	-
Cr_2HgS_2C	3.087	11.251	0	0	Metal	-	-
Cr_2MgO_2C	3.003	7.023	0.992	1.000	In. Semi.	0.736	30.773
Cr_2MgS_2C	3.272	8.306	0.343	0.678	In. Semi.	0.158	5.415
Cr_2SrO_2C	3.175	7.565	0.826	0.889	In. Semi.	0.603	25.495
Cr_2SrS_2C	3.432	8.716	0	0	Metal	-	-
Cr_2ZnO_2C	3.000	7.210	0.972	0.989	In. Semi.	0.713	30.282
Cr_2ZnS_2C	3.214	8.380	0.509	0.598	In. Semi.	0.328	14.861
Mo_2BaO_2C	3.332	8.302	0	0	Metal	-	-
Mo_2BaS_2C	3.499	9.848	0	0	Metal	-	-
Mo_2BeO_2C	2.776	8.166	0	0	Metal	-	-
Mo_2BeS_2C	3.309	8.252	0	0	Metal	-	-
Mo_2CaO_2C	3.307	7.489	0.779	1.000	In. Semi.	0.601	22.384
Mo_2CaS_2C	3.492	8.945	0.375	0.673	In. Semi.	0.065	1.713
Mo_2CdO_2C	3.108	9.637	0	0	Metal	-	-
Mo_2CdS_2C	3.263	11.08	0	0	Metal	-	-
Mo_2CuO_2C	3.149	7.570	0	0	Metal	-	-
Mo_2CuS_2C	3.296	8.703	0	0	Metal	-	-
Mo_2HgO_2C	3.111	9.850	0	0	Metal	-	-
Mo_2HgS_2C	3.282	11.368	0	0	Metal	-	-
Mo_2MgO_2C	2.949	8.187	0	0	Metal	-	-
Mo_2MgS_2C	3.413	8.645	0.502	0.576	In. Semi.	0.322	14.764
Mo_2SrO_2C	3.360	7.735	0.753	0.979	In. Semi.	0.571	20.979
Mo_2SrS_2C	3.514	9.288	0	0	Metal	-	-
Mo_2ZnO_2C	3.179	7.560	0	0	Metal	-	-

Mo_2ZnS_2C	3.363	8.732	0	0	Metal	-	-

Section S1. Computational Methodology

All calculations were performed using periodic DFT through the Vienna *Ab Initio* Simulation Package (VASP).[1-4] The projector-augmented wave (PAW) method was used to describe the interaction between the core and valence electrons.[5, 6] The PBE functional was used for geometry optimizations, whereas for electronic structure and optical calculations,[7] the hybrid Heyd-Scuseria-Ernzerhof functional (HSE06) including 25% screened Hartree–Fock exchange was employed.[8, 9] For all electronic calculations, a plane wave cutoff energy of 440 eV and a Γ-centred k-point meshes of 5×5×4 were used, with denser k-point meshes of 8×8×5 were applied for optical calculations to ensure that all important k-points were included. These parameters were necessary to converge the total energy of each system to within 10^{-5} eV□atom^{-1}. The atomic positions, a lattice shape, and cell volume were allowed to relax during geometry optimization, and the structures were considered to be converged once the forces on each atom were below 0.02 eV□Å^{-1}. The maximum photovoltaic efficiency and open-circuit voltage (V_{oc}) of an ideal absorber thin film were estimated using the spectroscopic limited maximum efficiency (SLME) metric introduced by Yu and Zunger,[10] based on the absorption calculated from HSE06 functional with tetrahedron correction.[11] The ionization potential was calculated using the core-level alignment approach of Wei and Zunger,[12] and the non-polar (110) surface was selected due to the absence of any dangling bonds. The work function was regarded as the ionization potential of metallic MAOX.

Section S2. Oxynitride and Sulnitride MAOX phase

A series of MAOX with A=Ca and M=Sc, Y, La, Cr, Mo were selected out as the representatives for the test of the metallicity of oxynitride and sulnitride MAOX, and the corresponding band structures are shown in Figure S1. As for the band structures of Sc_2CaO_2N, Sc_2CaS_2N, Y_2CaO_2N, Y_2CaS_2N, La_2CaO_2N, and La_2CaS_2N, energy levels are found crossing the Fermi level, indicating the conduction band is partially filled. Likewise, in the band structures of Cr_2CaO_2N, Cr_2CaS_2N, Mo_2CaO_2N, Mo_2CaS_2N, the band overlaps with another higher energy unoccupied conduction band. Therefore, all cases are metallic.

References

1 G. Kresse and J. Hafner, *Phys. Rev. B*, 1993, **47**, 558-561.

2 G. Kresse and J. Hafner, *Phys. Rev. B*, 1994, **49**, 14251-14269.

3 G. Kresse and J. Furthmuller, *Phys. Rev. B*, 1996, **54**, 11169-11186.

4 G. Kresse and J. Furthmuller, *Comp. Mater. Sci.*, 1996, **6**, 15-50.

5 P. E. Blöchl, *Phys. Rev. B*, 1994, **50**, 17953-17979.

6 G. Kresse and D. Joubert, *Phys. Rev. B*, 1999, **59**, 1758-1775.

7 J. P. Perdew, K. Burke and M. Ernzerhof, *Phys. Rev. Lett.*, 1996, **77**, 3865-3868.

8 J. Heyd, G. E. Scuseria and M. Ernzerhof, *J. Chem. Phys.*, 2003, **118**, 8207-8215.

9 J. Heyd, G. E. Scuseria and M. Ernzerhof, *J. Chem. Phys.*, 2006, **124**, 219906-219901.

10 L. P. Yu and A. Zunger, *Phys. Rev. Lett.*, 2012, **108**, 068701.

11 P. E. Blochl, O. Jepsen and O. K. Andersen, *Phys. Rev. B*, 1994, **49**, 16223-16233.

12 S. H. Wei and A. Zunger, *Appl. Phys. Lett.*, 1998, **72**, 2011-2013.